available at www.sciencedirect.com

ScienceDirect

journal homepage: www.elsevier.com/locate/biochempharm

Induction of G2/M phase arrest and apoptosis of human leukemia cells by potent antitumor triazoloacridinone C-1305

Ewa Augustin [a,*], *Anna Moś-Rompa* [a], *Anna Skwarska* [a], *Jacek M. Witkowski* [b], *Jerzy Konopa* [a]

[a] *Gdańsk University of Technology, Department of Pharmaceutical Technology and Biochemistry, Narutowicza St. 11/12, 80-952 Gdańsk, Poland*

[b] *Medical University of Gdańsk, Department of Pathophysiology, Gdańsk, Poland*

ARTICLE INFO

Article history:
Received 12 June 2006
Accepted 31 July 2006

Keywords:
Triazoloacridinones
C-1305
G2/M arrest
Apoptosis
Caspases
Mitochondria

ABSTRACT

In this study, we show that triazoloacridinone derivative C-1305, a potent antitumor compound, in human lymphoblastic (MOLT4) and promyelocytic (HL60) leukemia cells induces G2/M arrest followed by apoptosis. In both type of cells, C-1305 at biological relevant concentrations corresponding to EC_{90} value, induced a significant increase in the fraction of G2/M cells. The cell cycle perturbations were accompanied by the appearance of sub-G1 fraction, which can be considered as the apoptotic cells population. In both human leukemia cells apoptosis was additionally proved by appearance of DNA fragmentation, activation of caspase-3, PARP cleavage, externalization of phosphatydilserine as well as decrease of the mitochondrial transmembrane potential $\Delta\Psi_m$ and ATP depletion. Treatment of lymphoblastic MOLT4 cells with the C-1305 at EC_{90} concentration, caused massive death by apoptosis. Compared to MOLT4 cells, the capacity of HL60 cells to execute apoptosis after C-1305 treatment at equitoxic dose was significantly weaker, but very effective at high concentration (4× EC_{90}). These differences could originate from different sensitivity of both cell types to cytotoxic action of C-1305 (EC_{50} value for MOLT4 cells was 8 times lower than for HL60 cells and the EC_{90} value was 14 times lower, respectively). Collectively, these results show that C-1305 is a novel and potent compound which induces G2/M arrest and subsequent apoptosis of human leukemia cells. This strong ability to induce apoptosis of tumor cells support the view that C-1305 could be consider as a new potent and promising antitumor agent.

1. Introduction

Triazoloacridinones are a group of potent antitumor compounds, synthesized and developed at the Gdańsk University of Technology [1]. These compounds exhibited significant and clearly differentiated cytotoxic activity in vitro toward 64 human tumor cell lines in the NCI screening system (Bethesda, USA), and also displayed high antitumor activity against several experimental tumors in mice, especially leukemias and colon [1,2]. Among triazolacridinones, the most active derivative C-1305 (Fig. 1, panel A) was selected for extended preclinical trials.

The development of a new, active anticancer agent raises important questions about its mechanism of action. It was shown that C-1305 was a topoisomerase II poison that was able to induce cleavable complexes with topoisomerase II in cell-free system as well as in living cells [3]. Additional studies revealed that only the α isoform of topoisomerase II was covalently associated with DNA following exposure of

* *Corresponding author*. Tel.: +48 58 3471468; fax: +48 58 3471516.
E-mail address: augustin@chem.pg.gda.pl (E. Augustin).

0006-2952/$ – see front matter © 2006 Elsevier Inc. All rights reserved.
doi:10.1016/j.bcp.2006.07.035

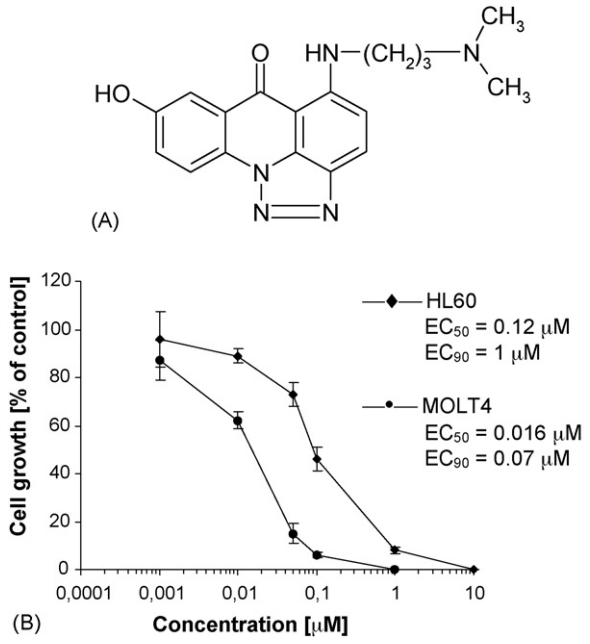

Fig. 1 – Chemical structure of triazoloacridinone derivative, C-1305 (panel A). Concentration-dependent growth inhibition of MOLT4 and HL60 cells by triazoloacridinone C-1305. Data are presented as mean ± S.D. of triplicate experiments (panel B).

living cells to C-1305 [4], in marked contrast to amsacrine—a classical topoisomerase II inhibitor which stimulated cleavable complexes with both isoforms. Triazoloacridinone C-1305 very strongly affected proliferation of cells lacking poly(ADP-ribose) polymerase-1 (PARP-1) [5]. This was in striking contrast with previous reports in which PARP-1 deficient cells were shown to be resistant to classical topoisomerase II inhibitors [6]. Triazoloacridinones like their structural analogues: imidazoacridinones [7] and mitoxantrone [8], after previous metabolic activation induce interstrand DNA crosslinking in tumor cells [9].

Treatment of tumor cells with various DNA-damaging agents, as well as topoisomerase-interacting agents or ionizing radiation, affects cell cycle progression, which often results in apoptosis [10,11].

Our study examined the effects of triazoloacridinone derivative C-1305 on the cell cycle progression and the induction of apoptosis. The high sensitivity of leukemia cells to C-1305 made us to choose the two human leukemia cell lines: lymphoblastic (MOLT4) and promyelocytic (HL60) leukemia cells as a model for our studies. Here, we provide evidence that C-1305, at EC_{90} concentration, induced G2/M arrest and subsequent apoptosis in both human leukemia cells studied.

2. Materials and methods

2.1. Chemicals and antibodies

Triazoloacridinone C-1305 was resynthesized by Barbara Horowska, PhD in the Department of Pharmaceutical Technology and Biochemistry at Gdańsk University of Technology. C-1305 was prepared as 10 mM stock solution in DMSO and kept at −20 °C until use. The stock solution was freshly diluted to the desired concentration just before use. Proteinase K was from Merck (Darmstadt, Germany), Annexin V-Fluos Staining Kit, terminal transferase, cobalt chloride, biotin-dUTP, TdT buffer were from Roche Molecular Biochemicals (Manheim, Germany). Mouse monoclonal antibody PARP (mAb-2) was from Calbiochem (San Diego, CA, USA), mouse monoclonal anti-β-actin antibody was from Sigma. All other reagents were of analytical grade and were purchased from Sigma.

2.2. Cell culture

MOLT4 (human lymphoblastic leukemia cells) and HL60 (human promyelocytic leukemia cells) were maintained in exponential growth at 37 °C in a humidified 5% CO_2 atmosphere in RPMI 1640 medium (GIBCO BRL Life Technologies) supplemented with 10% fetal bovine serum and antibiotics (100 μg/ml streptomycin, 100 IU/ml penicillin). Under these growth conditions the cell-doubling time was 12–14 h for MOLT4 cells and 20–24 h for HL60 cells.

2.3. Growth inhibition assay

Cell growth inhibition studies were assessed by cell counting using Coulter Counter, model ZB1. Briefly, cells (5×10^4 for MOLT4 and 10×10^4 for HL60) were seeded in six-well microculture plates with various drug concentrations for 48 h (for MOLT4 cells) or for 72 h (for HL60 cells). A dose response curves were plotted and concentrations that yielded 50% and 90% of inhibition of cell growth (EC_{50} and EC_{90}) were calculated.

2.4. Cell cycle analysis

Asynchronous MOLT4 and HL60 cells were exposed in the logarithmic phase of growth to C-1305 derivative at concentrations corresponding to EC_{90} value for 0–72 h. Cells were harvested by centrifugation for 5 min in 4 °C, at 1000 rpm, washed twice with ice-cold phosphate-buffered saline (PBS) and then were fixed in ice-cold 80% ethanol and frozen at −20 °C. Next, cells were centrifuged for 5 min in 4 °C, at 1000 rpm and washed twice with PBS. The supernatants were withdrawn and the cells were resuspended in 1 ml of DNA staining solution (20 μg/ml of propidium iodide PI, and 100 μg/ml of RNase A in PBS) for 30 min. Flow cytometric analyses were performed using a Becton Dickinson FACScan (San Jose, USA). At least 10 000 cells were collected and the data analysis was performed using the WinMDI software (J. Trotter, Scripps Research Institute, San Diego, USA).

2.5. Dual parameter cyclin B1/DNA measurements

Cyclin B1 was labeled by an direct immunofluorescence technique. MOLT4 and HL60 cells in the logarithmic phase of growth were exposed to the studied drug at EC_{90} concentrations for 12–72 h. Then, 1×10^6 cells were fixed with

ice-cold 80% ethanol for 2 h. Next, samples were centrifuged at 1000 rpm for 5 min, pellet was resuspended in 5 ml PBS, and the samples were stored for 5 min at room temperature. After centrifugation, supernatants were withdrawn and 5 ml PBS containing 1% bovine serum albumine (BSA) was added. The cells were centrifuged again, and the cell pellet was suspended in 1 ml 0.25% solution of Triton X-100 in PBS. Samples were kept on ice for 5 min, then 5 ml PBS was added to each sample and centrifuged at 1000 rpm for 5 min. Cells were incubated for 60 min at room temperature with gentle agitation, in the presence of the FITC-conjugated monoclonal antibody to mouse cyclin B1 (Santa Cruz Biotechnology, Inc., USA), at the appropriate dilution to obtain 2 μg of antibody in 1% BSA per sample. The negative control was incubated with FITC-conjugated goat anti-mouse IgG antibody (Sigma) diluted 1:30 in PBS containing 1% BSA. The cells were washed again, resuspended in 5 μg/ml of PI and 50 μg/ml of RNase A in PBS and incubated at room temperature for 30 min prior to FACS analysis.

2.6. Cytological techniques

For morphological determination of apoptotic cells, approximately 300 000 cells were spun onto a microscopic slide. The cytospin preparations were then fixed in Carnoy's fixative (glacial acetic acid:methanol, 1:3), rinsed once with PBS and stained with the DNA-intercalating fluorescent dye DAPI (0.1 μg/ml) for 5 min. Photographs were taken using OLYMPUS BX60 epifluorescence microscope. Cells that were shrunken and contained intensely staining nuclear fragments were regarded as apoptotic.

2.7. Genomic DNA isolation and agarose gel electrophoresis

Apoptotic degradation of DNA into the oligonucleosomal fragments was analyzed by agarose gel electrophoresis. For each incubation time with C-1305, 1×10^6 cells were washed twice with ice-cold PBS. After centrifugation, the cell pellet was suspended in lysis buffer (10 mM Tris–HCl, 10 mM EDTA, 10 mM NaCl, 0.5% SDS, pH 7.4) containing proteinase K (0.5 mg/ml) and incubated for 1 h at 50 °C. RNase A (2 mg/ml) was added and the mixture was incubated for an additional 2 h at 50 °C. NaCl was then added to 5 M concentration, and the DNA was precipitated by addition of three volumes of ice-cold ethanol and an overnight incubation at −20 °C. After centrifugation (14 000 rpm for 20 min at 4 °C), the entire pellet was dissolved in 20 μl of TE buffer (10 mM Tris–base, 1 mM EDTA, pH 8). The DNA samples were run on 1.8% agarose gel electrophoresis (8 mA overnight in TBE buffer: 45 mM Tris–base, 45 mM boric acid, 10 mM EDTA, pH 8) and visualized by ethidium bromide staining and photographed under ultraviolet illumination.

2.8. TUNEL assay (terminal deoxynucleotidyl transferase-mediated dUTP nick end-labeling assay)

The assay was performed using commercial kit (Roche Molecular Biochemicals, Manheim, Germany) and according to manufacturer's instructions. Following drug treatment, cells were collected by centrifugation and fixed in 1% formaldehyde in PBS for 15 min on ice. After centrifugation, the pellet was washed with PBS, resuspended in 70% ethanol and samples were stored overnight at −20 °C. After rehydration in PBS for 5 min cells were resuspended in 50 μl of reaction buffer (5 U terminal transferase, 2.5 mM cobalt chloride, 0.5 mM biotin-dUTP and TdT buffer containing 0.2 M potassium cocadylate, 25 mM Tris–HCl, 0.25 mg/ml BSA, pH 6.6) and incubated at 37 °C for 30 min. Cells were then washed with rinsing buffer (PBS containing 0.1% Triton X-100, 0.5% BSA), resuspended in 100 μl of staining buffer containing 2.5 μg/ml fluorescein isothiocyanate FITC-avidin, 4× SSC buffer, 0.1% Triton X-100 and 5% (w/v) non-fat dry milk and incubated for 30 min at room temperature in the dark. The pellets were then washed twice with rinsing buffer, resuspended in PBS containing 5 μg/ml propidium iodide and 100 μg/ml RNase A and incubated at room temperature for 30 min. The red (propidium iodide) and green (fluorescein) fluorescence were measured with FACScan flow cytometer.

2.9. Annexin V/PI flow cytometric analysis

Phosphatidylserine exposed on the outside of the apoptotic cells was determined by Annexin V-Flous Staining Kit (Roche Molecular Biochemicals, Manheim, Germany) and according to manufacturer's instructions. Briefly, following treatment with C-1305 for 0–72 h, cells (5×10^5) were harvested by low-speed centrifugation, washed twice with ice-cold PBS, pelleted and resuspended in 50 μl of Annexin V–FITC diluted in binding buffer containing propidium iodide. FITC-conjugated Annexin V and PI were added at manufacturer's recommended concentrations. Cells were incubated for 15 min at room temperature in the dark. After incubation, cell suspensions were diluted with 0.35 ml of binding buffer and analyzed by flow cytometry within 1 h. Flow cytometry and data analysis were performed as described previously.

2.10. Measurement of mitochondrial membrane potential ($\Delta\Psi_m$)

To measure mitochondrial membrane potential ($\Delta\Psi_m$), mitochondria were selectively probed with potential-sensitive JC-1 (5,5′,6,6′-tetrachloro-1,1′,3,3′-tetraethylbenzimidazolyl-carbocyanine iodide, Sigma, St Luis, MO). After treatment, cells (5×10^5) were harvested and washed twice with PBS and incubated with medium containing JC-1 (10 μg/ml) for 15 min at room temperature in the dark. Finally, cells were washed and resuspended in 1 ml of PBS for flow cytometry analysis. Events with low red and high green fluorescence were regarded as the cells with low $\Delta\Psi_m$.

2.11. Apoptosis detection by active caspase-3 measurement

Activated caspase-3 as a marker for cells undergoing apoptosis was determined by the Active Caspase-3 Apoptosis Kit (BD Pharmingen, San Diego, CA). Briefly, untreated and C-1305-treated cells (1×10^6) were washed twice with cold PBS, then fixed and permeabilized using Cytofix/Cytoperm™ for 20 min

on ice, pelleted and washed with Perm/Wash™ Buffer. Cells were then stained with anti-active caspase-3 mAb using 20 μl/1×10^6 cells for 30 min at room temperature in the dark. Following incubation with antibody cells were washed with Perm/Wash™ buffer, resuspended in Perm/Wash™ buffer and analyzed by flow cytometry.

2.12. Western blot for PARP

Cells were lysed on ice for 30 min in radioimmunoprecipitation assay buffer (150 mM NaCl, 50 mM Tris–HCl, 1% Igepal CA630, 5 mM EDTA, 0.1% SDS, 0.5% sodium deoxycholate, 50 mM NaF, 1 mM PMSF) with freshly added protease inhibitor mixture (Calbiochem, San Diego, CA). Cell lysates were centrifuged at 14 000 rpm for 15 min at 4 °C. Protein concentration was determined using Bio-Rad protein assay (Bio-Rad Laboratories, Hercules, CA). Samples were mixed with Laemmli buffer, denaturated at 100 °C for 5 min, and 60 μg of total proteins was subjected to SDS-PAGE, transferred onto nitrocellulose membrane and blocked with 5% non-fat milk in TBS-T buffer (150 mM NaCl, 10 mM Tris (pH 7.4) and 0.05% Tween-20) at room temperature for 2 h. The membrane was incubated with mouse monoclonal anti-PARP antibody (Calbiochem, San Diego, CA) diluted at 1:1000 in TBS-T buffer containing 0.5% non-fat dry milk at 4 °C overnight with rocking. After washing with TBS-T three times at 15 min each, membrane was incubated with horseradish peroxidase-conjugated secondary antibody diluted at 1:10 000 in TBS-T for 1 h at room temperature. Antigen was detected using the enhanced chemiluminescence western blotting detection system (Pierce Biotechnology, Rockford, IL) according to the protocol of the manufacturer. Equal protein loading was confirmed by rehybridization of membrane and reprobing with anti-β-actin antibody.

2.13. Measurement of intracellular ATP

Cellular ATP levels were measured in supernatants of tumor cells homogenized in 30% perchloric acid and centrifuged at 14 000 rpm at 4 °C, for 5 min using a luciferin/luciferase assay [12]. The ATP assay was validated in each experiment using exogenous ATP standards. Background readings were substracted from both standards and samples. A 100 μl aliquot of sample was mixed with 100 μl of luciferase, and the light output was recorded on the luminometer (Dynatech, Denkendorf, Germany). All samples were run in triplicate. Standard curves for ATP were prepared for each experiments. The amount of ATP was quantitated by comparing light output from an unknown sample with that from a standard solution of ATP.

3. Results

3.1. Inhibition of the proliferation of MOLT4 and HL60 cells by C-1305

The effect of C-1305 on cellular proliferation of MOLT4 and HL60 cells was estimated by cell counting using a Coulter Counter. A 48- or 72-h exposure to C-1305 dramatically decreased proliferation of MOLT4 and HL60 cells, respectively, in a concentration-dependent manner (Fig. 1, panel B). The estimated concentration required to inhibit cell growth by 50% (EC_{50}) and 90% (EC_{90}) demonstrated that HL60 cells exhibited lower sensitivity to C-1305 than MOLT4 cells.

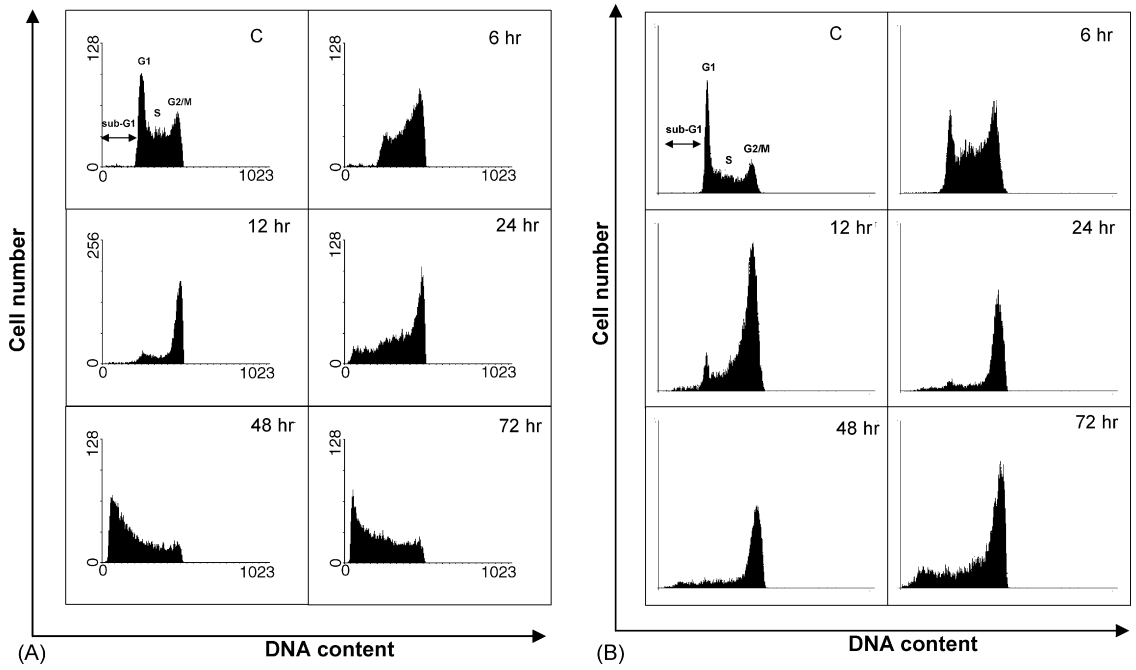

Fig. 2 – Cell cycle distribution determined by flow cytometry in MOLT4 cells treated with 0.07 μM (1× EC_{90}) C-1305 (panel A) and in HL60 cells treated with 1 μM (1× EC_{90}) C-1305 (panel B) for the time indicated. Histograms show number of cells per channel (y-axis) vs. DNA content (x-axis). Data correspond to a representative experiment out of three, which gave similar results.

Table 1 – Percentage of sub-G1 and cell cycle distribution (%) of MOLT4 and HL60 cells treated with 0.07 μM (1× EC_{90}) or 1 μM (1× EC_{90}) C-1305 respectively, for the time indicated

Cell line	Time of treatment (h)	Cell cycle distribution (%)			
		Sub-G1 ± S.D.	G1 ± S.D.	S ± S.D.	G2/M ± S.D.
MOLT4	Control	0.51 ± 0.020	37.19 ± 0.90	39.6 ± 1.0	23.30 ± 0.76
	6	1.04 ± 0.066	15.47 ± 0.70	47.33 ± 0.90	36.84 ± 0.77
	12	2.02 ± 0.27	8.94 ± 0.48	19.44 ± 0.29	70.33 ± 0.57
	24	16.14 ± 0.90	13.95 ± 0.40	33.9 ± 1.2	36.71 ± 0.36
	48	61.4 ± 1.4	13.84 ± 0.67	17.56 ± 0.82	7.60 ± 0.27
	72	52.37 ± 0.63	16.54 ± 0.76	22.9 ± 1.0	8.8 ± 0.52
HL60	Control	0.62 ± 0.15	43.9 ± 1.3	35.2 ± 1.0	20.83 ± 0.89
	6	0.84 ± 0.04	21.5 ± 1.1	44.7 ± 1.4	33.5 ± 1.5
	12	2.39 ± 0.43	8.81 ± 0.41	30.76 ± 0.56	58.6 ± 1.1
	24	4.43 ± 0.29	6.52 ± 0.48	14.19 ± 0.17	74.7 ± 2.1
	48	8.95 ± 0.61	5.96 ± 0.34	15.82 ± 0.76	68.91 ± 0.68
	72	15.15 ± 0.88	6.85 ± 0.55	23.53 ± 0.89	54.02 ± 0.48

Data correspond to a representative experiment out of three, which gave similar results.

3.2. *Effect of C-1305 on the cell cycle progression*

To establish the effect of C-1305 on the progression of MOLT4 and HL60 cells through the cell cycle, cells were cultured for various times (6, 12, 24, 48, 72 h) in the presence of C-1305 at EC_{90} concentration and analyzed by flow cytometry. Fig. 2 shows typical DNA histograms obtained from FACS analysis and detailed data concerning the percentage of sub-G1 cells and cell cycle distribution of MOLT4 and HL60 cells treated with C-1305 for various times were shown in Table 1. Compared to the control (untreated cells), MOLT4 cells accumulated in the S phase by 6 h of treatment with C-1305 at a concentration of 0.07 μM (1× EC_{90}). This effect was transient, and by 12 h there was an increase in the number of cells in the G2/M phase (70%), with corresponding decrease in the G1- and S-phase fraction. After prolonged drug incubation (24 h or longer), G2/M arrest was also accompanied by an increase in the sub-G1 region of cells with a fractional DNA contents, which was typical for late stages of apoptosis (52% of sub-G1 cells after 72 h of treatment with C-1305). Changes in cell cycle distribution of HL60 cells following treatment with C-1305 at concentration of 1 μM (1× EC_{90}) were evident after 6 h of treatment, where transient S-phase accumulation was observed. At longer incubation times (12 or 24 h), the majority of cells remained in a G2/M cell cycle arrest (58% and 74%, respectively). G2/M arrested cell population slowly decreased with prolonged drug exposure (48, 72 h). This was accompanied by the appearance of the small population of the cells with sub-G1 levels of DNA (9% after 48 h and 15% after 72 h). However, the incubation of the cells with increased drug concentration (4× EC_{90}) significantly increased the percentage of sub-G1 cells (60% after 72 h) (data not shown).

3.3. *Effect of C-1305 on cyclin B1 expression*

To investigate the cellular events responsible for the accumulation of MOLT4 and HL60 cells in the G2/M phase after exposure to C-1305 at EC_{90} concentrations, we evaluated cyclin B1 expression after different time of incubation. Cyclin B1 is a well-known marker of G2-M transition, which expression is essentially limited to late S and G2 phase, and its degradation occurs at the meta-to-anaphase transition [13]. In asynchronously growing MOLT4 and HL60 cells (Fig. 3), cyclin B1 significantly accumulated after 12 h of exposure to C-1305 and the fraction of cyclin B1-expressing cells increased in parallel with the increase of the fraction of G2/M phase cells. In MOLT4 cells the level of cyclin B1 positive cells decreased after 24 h of treatment with C-1305. This was accompanied with gradual loss of G2/M arrested cells as well as concomitant appearance of condensed chromosomes (Fig. 4, panel A). In the case of HL60 cells the level of cyclin B1 positive cells was highest after 12 h of treatment. After 24 h of C-1305 treatment population of cyclin B1 positive cells slightly decreased. Significant decrease of cyclin B1 positive cells was observed after 48 and 72 h, however condensed chromosomes were not detected (Fig. 4, panel B).

3.4. *Effect of C-1305 on morphological changes of the cells*

The appearance of sub-G1 population of MOLT4 and HL60 cells treated with C-1305 was accompanied by characteristic

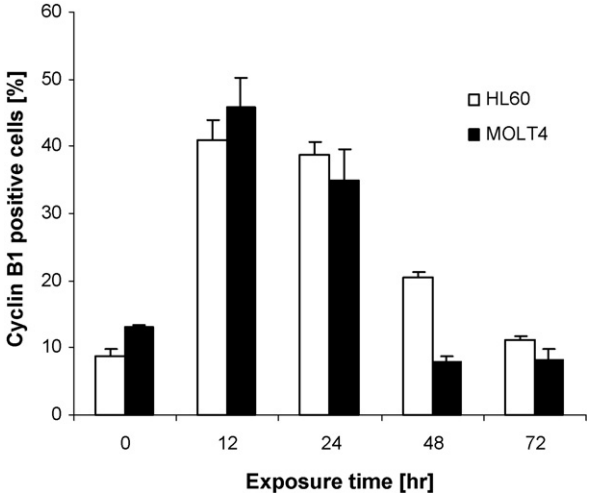

Fig. 3 – Quantitative representation of the flow cytometry data with fraction of cyclin B1 positive MOLT4 and HL60 cells treated with C-1305 at EC_{90} concentrations. Data are presented as mean ± S.D. of triplicate experiments.

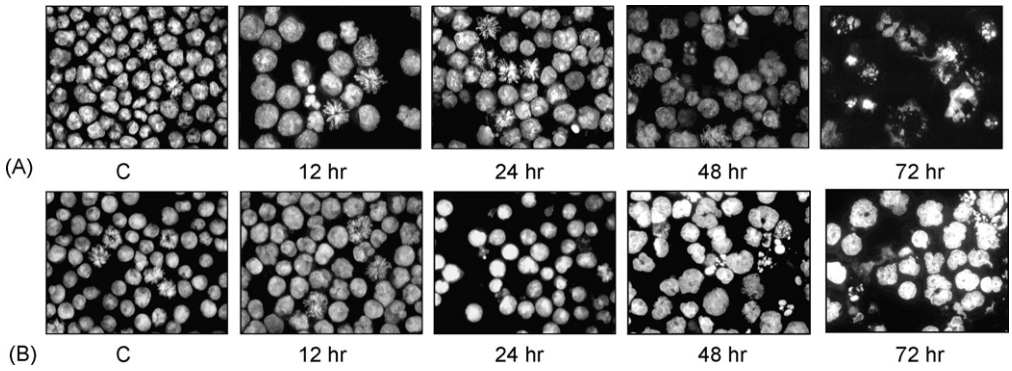

Fig. 4 – Cell morphology of MOLT4 (panel A) and HL60 (panel B) cells exposed to C-1305 at EC_{90} concentrations for the indicated times. Cells that were shrunken and contained regions of intense chromatin staining were considered as apoptotic. Cytospin preparations were stained with DAPI and viewed under 400× magnification.

morphological changes. In parallel to cytometric studies, the cells loaded with DAPI were observed under the fluorescence microscope to asses drug-induced changes of the cell morphology. A shown in Fig. 4, untreated control cells exhibited unchanged morphology, characteristic for leukemia cells. MOLT4 and HL60 cells treated with C-1305 at EC_{90} concentrations for 12 h had much larger nuclei than the control cells, because of the induction of the G2/M arrest. In the case of MOLT4 cells, few apoptotic cells were observed after 24 h of incubation with the drug, and the mitotic chromosomes were also visible. After 48 h of C-1305 treatment, the population of multinucleated cells appeared. Significant morphological changes, e.g. chromatin condensation and nuclear degradation, which was indicative of apoptotic cell death were noted in MOLT4 and HL60 cells treated for 48 and 72 h. Together with the appearance of hypodiploid cells (sub-G1 fraction) seen in flow cytometric analyses, these morphological observations confirm the presence of considerable amount of apoptotic MOLT4 cells and lower amount of HL60 cells, following treatment with C-1305 at EC_{90} concentrations.

3.5. *DNA fragmentation*

Cell cycle analysis revealed that C-1305 induced G2/M arrest followed by the appearance of sub-G1 nuclei in both studied cell lines. Furthermore, treatment with C-1305 also resulted in the internucleosomal DNA fragmentation which was seen as characteristic DNA pattern (''ladder'') on agarose gels. As can be seen in Fig. 5, panel A, C-1305 at EC_{90} concentration produced internucleosomal DNA fragmentation after 48 h and 72 h in MOLT4 cells. A weak ladder like pattern, typical of DNA cleavage between nucleosomes, has been also observed in HL60 cells after 48–72 h incubation with C-1305 (data not shown).

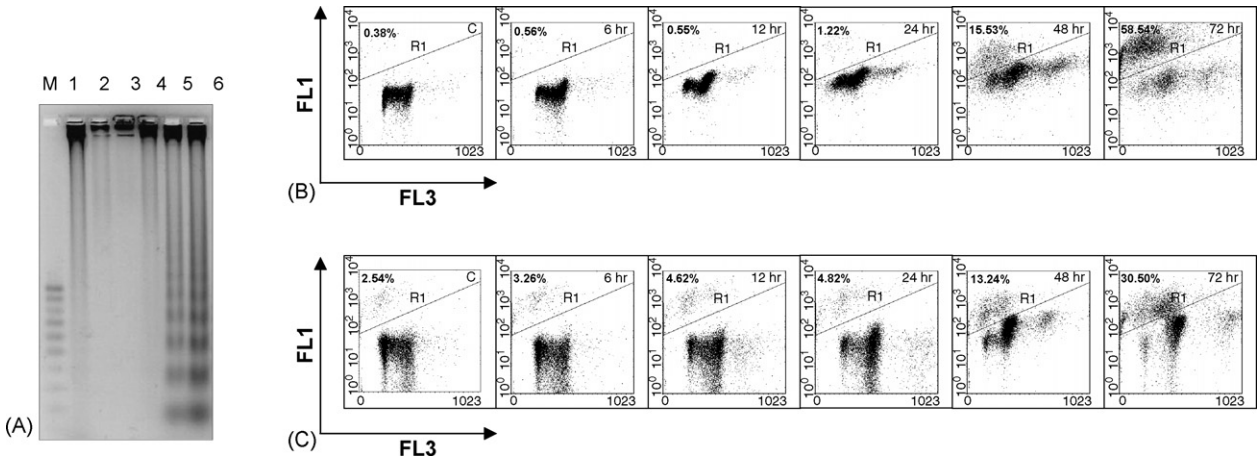

Fig. 5 – DNA fragmentation in MOLT4 cells treated with 0,07 μM C-1305 for the times indicated. M: 100–1000 bp DNA marker; lane 1: untreated cells; lanes 2–6: 6, 12, 24, 48, 72 h of incubation. Internucleosomal DNA fragments were resolved by gel electrophoresis in a 1.8% agarose gel and visualized by ethidium bromide staining. Experiments were performed three times with consistent results (panel A). TUNEL assay for MOLT4 cells (panel B) and HL60 cells (panel C). Cells were exposed to the drug at EC_{90} concentrations for the time indicated and stained for DNA fragmentation (biotinylated dUTP incorporation, *y*-axis) and DNA content (propidium iodide, *x*-axis) and analyzed by biparameter flow cytometry. Gated regions were TUNEL positive populations. Data represent one experiment from a series of three similar experiments that gave equivalent results.

To further confirm apoptotic degradation of DNA and to determine whether the DNA fragmentation observed in the treated cells occurred in particular phase of the cell cycle, the TUNEL assay was carried out. In this assay, DNA strand breaks were labeled with biotynylated dUTP and terminal transferase followed by dual staining with avidin–FITC conjugate and propidium iodide. As shown in Fig. 5, panels B and C, the cells with low level of fragmented DNA could be observed 24 h after treatment of MOLT4 and HL60 cells with C-1305 at EC_{90} concentrations. Starting from 48 h of incubation, the fraction of cells with fragmented DNA rapidly increased (15% in the case of MOLT4 cells and 13% in the case of HL60 cells). After prolonged incubation time (72 h) the fraction of cells with fragmented DNA achieved level of 58% in MOLT4 cells and 30% in HL60 cells. Biparametric flow cytometry analysis showed that DNA fragmentation after 72 h C-1305 exposure preferentially occurred in G2/M region in HL60 cells. In the case of MOLT4 cells, DNA degradation appeared from all phases of the cell cycle.

3.6. *Loss of plasma membrane asymmetry*

To further characterize apoptosis induced by C-1305, a biparametric cytometric analysis was performed using PI and Annexin V-FITC which stain DNA and phosphatidylserine (PS) residues, respectively. The phospholipid-binding protein Annexin V has a high affinity for PS and can bind to cells with externally exposed PS. Positive staining with fluorescently labeled Annexin V correlates with loss of membrane polarity during apoptosis, but precedes the complete loss of membrane integrity that accompanies later stages of cell death resulting form either apoptosis or necrosis [14]. In contrast, PI can only enter cells after loss of membrane integrity. Thus, dual staining with Annexin V and PI allows clear discrimination between unaffected cells (Annexin V negative, PI negative), early apoptotic cells (Annexin V positive, PI negative), and late apoptotic cells (Annexin V positive, PI positive).

After the drug treatment, cells were labeled with these two dyes, washed and resulting red (PI) and green (FITC) fluorescence was monitored by flow cytometry. The results obtained from MOLT4 cells are displayed in Fig. 6, panel A. As indicated on the figure, cells remained largely unaffected for the first 12 h of C-1305 treatment. The percentage of Annexin V positive cells increased after prolonged incubation with C-1305. After 24 h of incubation 11.8% of the cells stained positively with Annexin V (early stage of apoptosis) and only 1.9% with Annexin V and PI (late stage of apoptosis). After 48 h of treatment the percentage of Annexin V positive cells reached 22.3%, but 17.3% of the cells were also colored with PI. The fraction of Annexin V positive cells and PI positive cells increased dramatically after 72 h of incubation with C-1305 (36.1% and 39.8%, respectively). The similar experiments were performed with HL60 cells. As shown in Fig. 6, panel B only 10.4% of the cells showed Annexin V binding after 72 h of incubation with the drug. Proportion of late-stage apoptotic cells (Annexin V positive, PI positive) increased after 72 h of C-1305 treatment and reached 8.4%. However, increase of C-1305 concentration to 4 μM (4× EC_{90}) resulted in dramatically

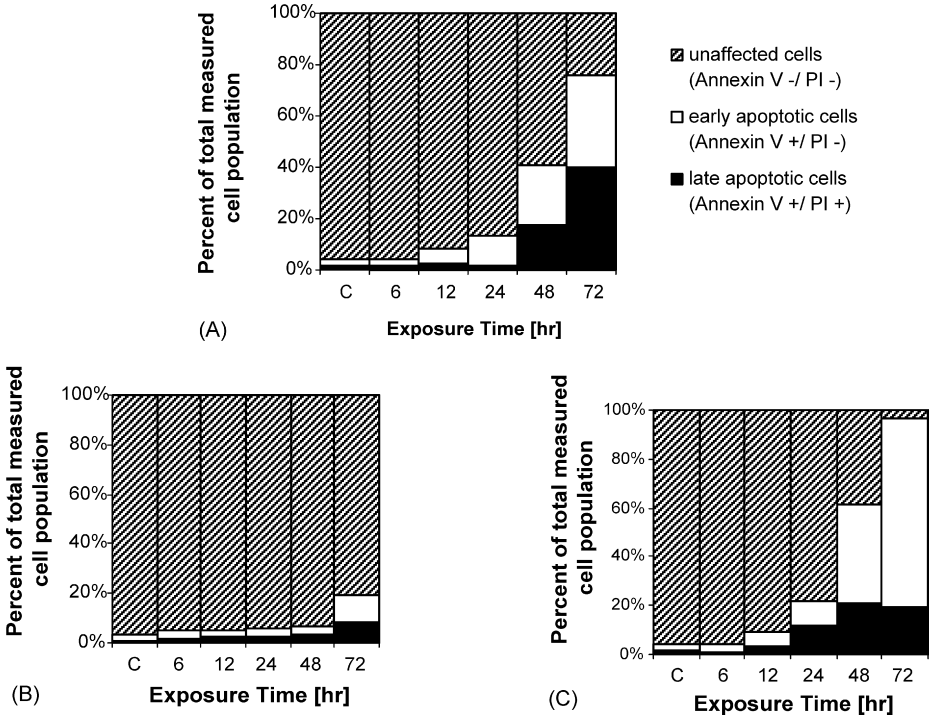

Fig. 6 – Phosphatidylserine externalization in C-1305-treated MOLT4 cells at 1× EC_{90} concentration (panel A) and HL60 cells in 1× EC_{90} concentration (panel B) and 4× EC_{90} concentration (panel C). Percentages of the total cell population were plotted for untreated cells (Annexin V negative, PI negative), early apoptotic cells (Annexin V positive, PI negative), and late apoptotic cells (Annexin V positive, PI positive). One representation of three independent flow cytometric analyses at indicated times of treatment.

increase of Annexin V positive and PI positive cells (77.1% and 19.1%, respectively after 72 h treatment) (Fig. 6, panel C).

3.7. Decrease of mitochondrial membrane potential $\Delta\Psi_m$

Mitochondria play a crucial role in apoptosis [15]. One of the major parameters of mitochondrial dysfunction is the decrease of mitochondrial membrane potential $\Delta\Psi_m$ that constitutes an irreversible event in the apoptotic process [16]. $\Delta\Psi_m$ was monitored in C-1305 treated leukemia cells using the cationic JC-1 dye, which is considered as a reliable probe to assess $\Delta\Psi_m$ changes [17]. JC-1 selectively enters to mitochondria and has the unique property of forming red-fluorescent JC-1 aggregates under high mitochondrial $\Delta\Psi_m$. As shown in Fig. 7, panel A, a time-dependent increase in the proportion of MOLT4 cells with a reduced $\Delta\Psi_m$ was noted following C-1305 treatment, relative to a control (untreated) cells. No change in the mitochondrial membrane potential was observed in MOLT4 cells at early time points of treatment (0–12 h); whereas the population of cells with low $\Delta\Psi_m$ slightly increased after 24 h of exposure to C-1305. The effect was further intensified after 48–72 h of incubation with the drug. Flow cytometric determinations indicated that HL60 cells exposed to C-1305 did not exhibit significant changes in mitochondrial membrane potential $\Delta\Psi_m$. The small population of HL60 cells with a reduced $\Delta\Psi_m$ was only noted after 72 h of incubation with C-1305 (Fig. 7, panel B).

3.8. Activated caspase-3 as a marker of cells undergoing apoptosis

The caspase family of proteases are involved in the initiation and execution stages of apoptosis. Among these, caspase-3, appears to be essential for executive stage of apoptosis [18], and thus, the caspase-3 activity in MOLT4 and HL60 cells treated with C-1305 at EC_{90} concentrations was examined. A convenient and broadly accepted method to study the activity of caspase-3 during apoptosis involves intracellular antigen staining with antibody against active form of caspase-3. Following fixation, permeabilization and staining, the amount of active caspase-3 can be measured by flow cytometry. In the case of MOLT4 cells (Fig. 8, panel A), after 12 and 24 h of treatment with C-1305, we did not observed active caspase-3. However, 48 h of treatment induced significant increase in number of cells with active caspase-3 (about 40%), and after 72 h of incubation the percentage of cells expressing active caspase-3 reached about 65%. Compared to MOLT4 cells, the percentage of HL60 cells expressing active caspase-3 after C-1305 treatment, was very low. After 72 h of incubation with the drug, only about 5% of cells displayed active caspase-3.

We also examined PARP proteolysis as a marker of caspase activation. Poly(ADP-ribose) polymerase (PARP) is a highly conserved nuclear enzyme involved in DNA repair and activated in response to DNA damage [19,20]. It is also a preferential substrate for caspase-3 which is cleaved by this protein into 89- and 24-kDa fragments during apoptotic mode of cell death. Fig. 8, panel B showed PARP cleavage in cells treated with C-1305 at EC_{90} concentrations for up to 72 h. In MOLT4 cells C-1305 was very efficient in inducing PARP cleavage, as reflected by the intensity of the 89 kDa PARP fragments which were clearly visible after 48 and 72 h of incubation with the drug. In HL60 cells, C-1305 induced caspase-3 mediated PARP cleavage, but with a much lower efficiency.

It is worth to point out that in MOLT4 cells the activation of caspase-3 and PARP proteolysis were observed concomitantly with the dissipation of $\Delta\Psi_m$. Compared to MOLT4 cells, the small population of HL60 cells with dissipated mitochondrial inner potential ($\Delta\Psi_m$) coincided well with the small population of the cells with active caspase-3 and with the efficiency of PARP cleavage induced by C-1305.

3.9. ATP depletion during C-1305 induced apoptosis

Recent studies suggest that mitochondrial damage appears to be a critical step of apoptotic cascade. One of the effects of the

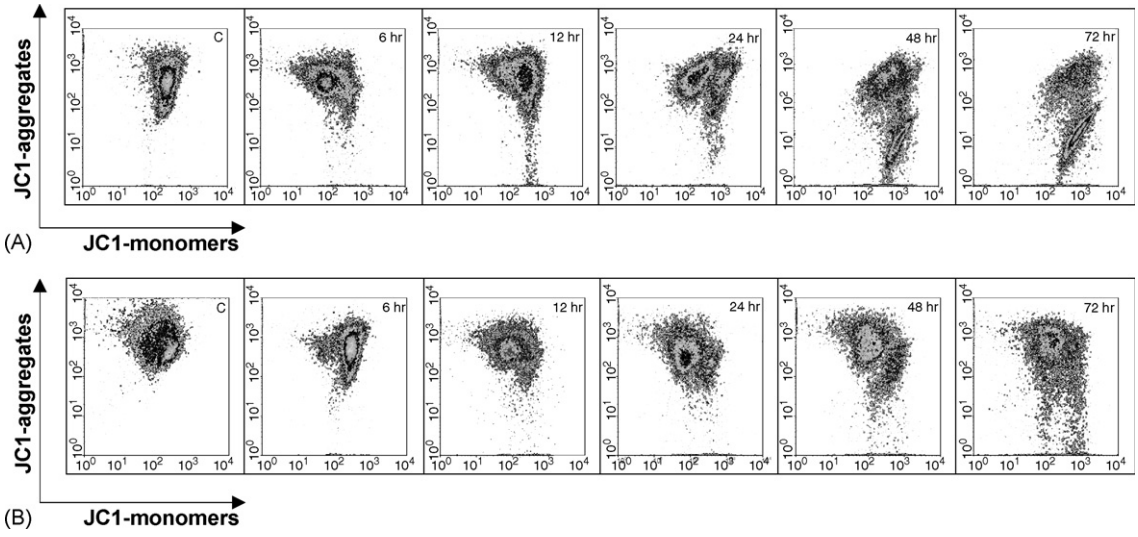

Fig. 7 – Flow cytometric analysis of changes in mitochondrial membrane potential ($\Delta\Psi_m$) in MOLT4 (panel A) and HL60 (panel B) cells treated with C-1305 at EC_{90} concentrations. The loss of $\Delta\Psi_m$ was evaluated by JC-1 staining and was seen as a shift to lower JC-1 red fluorescence. Data correspond to a representative experiment out of three, which gave similar results.

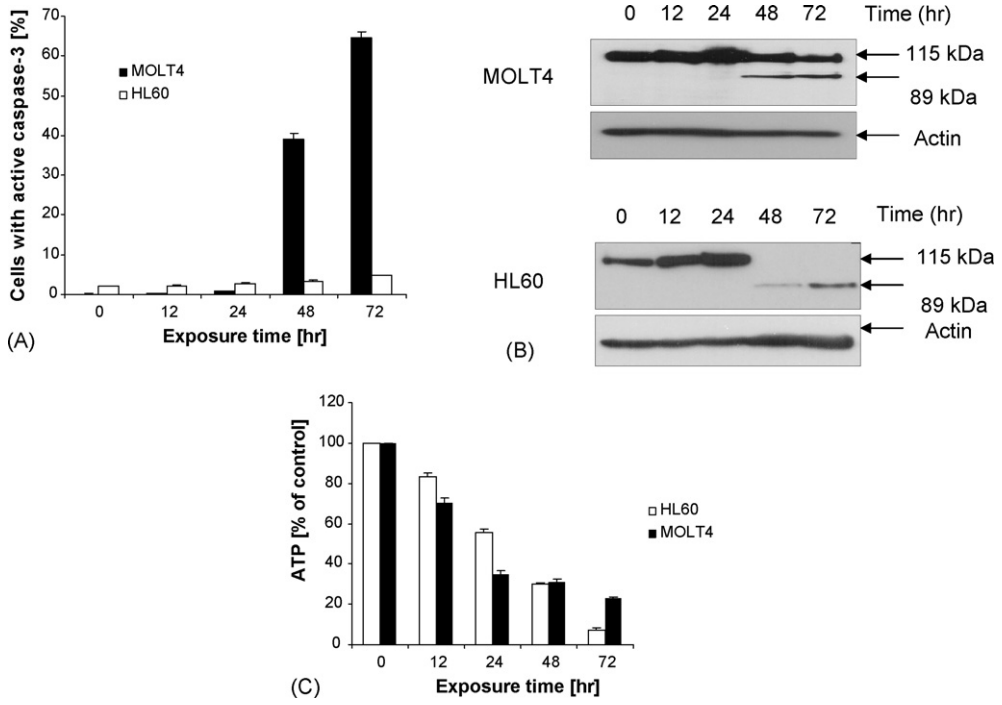

Fig. 8 – Quantitative representation of the flow cytometry data with fraction of caspase-3 positive MOLT4 and HL60 cells treated with C-1305 at EC_{90} concentrations. Data are presented as mean ± S.D. of triplicate experiments (panel A). Induction of PARP cleavage in MOLT4 and HL60 cells by C-1305 at EC_{90} concentrations. Western blot was used to detect the cleavage of full-length PARP (115 kDa band) into 89 kDa fragment in untreated cells and treated with C-1305 for the time indicated. Whole cell lysates were subjected to SDS-PAGE followed by blotting with an anti-PARP monoclonal antibody. Results are representative of two independent experiments (panel B). ATP depletion in MOLT4 and HL60 cells treated with C-1305 at EC_{90} concentrations. Time-course of intracellular ATP level was determined by luciferin–luciferase assay. Data are presented as mean ± S.D. of triplicate experiments (panel C).

mitochondrial damage is ATP depletion [15] which could also result from increasing poly(ADP-ribosyl)ation of acceptor proteins as reaction to DNA damage [21]. Thus, it was interesting to evaluate the effect of C-1305 on the ATP level in MOLT4 and HL60 cells. In the case of both cell lines, decrease of the ATP level was evident and was detectable after 12 h of incubation with C-1305 at EC_{90} concentrations (Fig. 8, panel C). The effect was further intensified after prolonged times of incubation with the drug. In MOLT4 cells this effect was correlated with the reduction of mitochondrial membrane potential ($\Delta\Psi_m$) which dissipation started also from 12 h of C-1305 treatment. In contrast, in HL60 cell line, despite of slight dissipation of $\Delta\Psi_m$, we observed an evident depletion of cellular ATP content.

4. Discussion

Triazoloacridinone C-1305 inhibits cleavable complexes of topoisomerase II with DNA [3] and induces formation of interstrand crosslinks in DNA of tumor cells, after previous metabolic activation [9]. It is well known that topoisomerase II inhibitors, e.g. etoposide [22], anthracyclines and the majority of antitumor interstrand DNA crosslinking agents [23], induce cell cycle arrest in the G2/M phase as their first biological effect. It is also well proved that several inhibitors of topoisomerase II, e.g. anthracyclines [24] and other anticancer drugs [25] induce apoptosis in tumor cells. However, authors did not pay attention if this final biological effect appeared at concentrations at which G2/M arrest should have been observed.

Two human leukemia cell lines: MOLT4 and HL60 were used to show the effect of C-1305 on the cell cycle progression and apoptosis. The studies were performed mainly at EC_{90} concentration of the drug that caused 90% of inhibition of cells proliferation, however some studies were performed also at concentration of the drug corresponding to 4× EC_{90} value. Sensitivity of both type of cells to cytotoxic action of C-1305 were different (EC_{50} value for MOLT4 cells was 8 times lower than for HL60 cells and EC_{90} value was 14 time lower, respectively). It is worth to point out that leukemia MOLT4 cells were the most sensitive to C-1305 among all 64 tumor cell lines in NCI (Bethesda, USA) in vitro screening system (unpublished data).

As revealed from cell cycle analysis, both cell lines treated with the EC_{90} concentrations of the drug showed a transient delay in S phase of the cell cycle, with the maximal S-phase fraction after 6 h, followed by accumulation of cells in G2/M after prolonged drug incubation (24 h and longer). G2/M arrest was accompanied by an increase in the sub-G1 region of cells, considered as a marker of cell death by apoptosis. Quantitation of the sub-G1 material indicated that this population

represented 60% of the MOLT4 cells and only 15% of the HL60 cells (Fig. 2). However, in the case of HL60 cells, treatment with the 4× EC_{90} concentration of C-1305 resulted in significant increase of sub-G1 population (60% after 72 h).

To further analyze the molecular mechanism by which C-1305 causes the cell cycle arrest, we evaluated cyclin B1 expression. Cyclin B1 together with cdc2 kinase create well-known complex, which is one of the major regulatory elements governing the G2 to M progression [26]. We found that cyclin B1 significantly accumulated after 12 or 24 h of C-1305 treatment of MOLT4 and HL60 cells, respectively (Fig. 3), consistently with the cell doubling-time, in parallel with the increase of the fraction of G2/M cells of both leukemia cell lines. In MOLT4 cells the level of cyclin B1 positive cells decreased after 24 h of drug treatment which was accompanied with loss of G2/M arrested cells as well as concomitant appearance of condensed chromosomes. Thus, these data suggest that at least part of G2 arrested cells may traverse into mitosis. After prolonged drug incubation (48 and 72 h) decreased expression of cyclin B1 was clearly visible. Compared to MOLT4 cells, in HL60 cells the level of cyclin B1 positive cells was still high after 24 h of drug treatment. Dramatic decrease of cyclin B1 positive cells was observed after prolonged incubation (48 and 72 h), however we did not observed condensed chromosomes during microscopic examination. Thus, compared to MOLT4 cells, G2 arrest was more stable, cells did not traverse into mitosis.

Apoptosis is a fundamental process essential for both development and maintenance of tissue homeostasis and this process was first recognized by Kerr et al. [27]. The morphological changes of apoptosis include membrane blebbing, cell shrinkage, chromatin condensation, DNA fragmentation and formation of apoptotic bodies [28]. We observed that the appearance of the sub-G1 population after C-1305 treatment was accompanied by these characteristic for apoptosis morphological changes, as indicated by DAPI staining (Fig. 4). Additionally, in MOLT4 cells, mitotic chromosomes were easily visible after 24 h of drug treatment and after 48 h we observed appearance of multinuclei which are the hallmark of mitotic catastrophe [29]. The appearance of condensed chromosomes and multinuclei as well as decrease of the population of cyclin B1 positive cells suggests, that part of MOLT4 cells may undergo mitotic catastrophe. However, further studies are needed to evaluate the induction of this type of cell death by C-1305 in MOLT4 cells.

Apoptosis is an active process that ultimately leads to the activation of endonucleases and cleavage of DNA into fragments of about 180–200 base pairs [30]. Exposure of leukemia cells to C-1305 results in a cleavage of cellular DNA in a internucleosomal pattern, characteristic for apoptotic cell death (Fig. 5, panel A). However, compared to MOLT4 cells, in HL60 cells this pattern was somewhat weaker (data not shown). The DNA fragmentation in MOLT4 and HL60 cells were also confirmed by TUNEL assay (Fig. 5, panels B and C). After prolonged incubation time (72 h) the fraction of cells with fragmented DNA were 58% in MOLT4 cells and were smaller (30%) in HL60 cells. DNA cleavage after this prolonged incubation with C-1305 preferentially occurred from G2/M region in HL60 cells, however for MOLT4 cells DNA fragmentation was observed from each phase of the cell cycle.

One of the early events of apoptosis is translocation of phosphatidylserine (PS), a phospholipid normally confined to the cytoplasmic face of the plasma membrane, to the cell surface in most cell types and by many apoptotic stimuli. Externalization of PS to the cell surface marks the apoptotic cells to be recognized by neighboring cells or macrophages, facilitating the noninflammatory removal of dying cells by phagocytosis [31]. The induction of apoptosis of MOLT4 and HL60 cells by C-1305 was also confirmed by the loss of membrane asymmetry (Annexin V positivity). Annexin V/PI assay allows to quantitation of the apoptotic process. In MOLT4 cells the significant increase in apoptotic cell population (76%) was observed after 72 h of C-1305 treatment (Fig. 6, panel A). These data correlated with those obtained from cell cycle analysis, where 52% of the population represented the cells with sub-G1 DNA content (Table 1). Compared to MOLT4, in HL60 cells, the fraction of apoptotic cells reached only 20% after 72 h of drug treatment (Fig. 6, panel B). In parallel, as revealed by cell cycle analysis, the population of cells with sub-G1 DNA content was about 15% (Table 1). However, treatment with 4× EC_{90} concentration of C-1305 resulted in dramatic increase of apoptotic cells (about 96%) (Fig. 6, panel C) and the fraction of the cells with sub-G1 DNA content was also increased.

Mitochondria play an important role in regulating apoptosis. One of the early apoptotic events is the alteration of the integrity of mitochondrial membranes consisting of inner and outer membrane. Collapse of the mitochondrial membrane potential ($\Delta\Psi_m$) accompanies or is a prerequisite for rapid mitochondria-mediated apoptosis [15,16]. Our studies demonstrated significant decrease of the mitochondrial membrane potential ($\Delta\Psi_m$) after C-1305 treatment in MOLT4 cells and only a slight decrease of $\Delta\Psi_m$ in HL60 cells, in a time-dependent manner (Fig. 7). Induction of apoptosis in HL60 cells without significant changes in $\Delta\Psi_m$ was demonstrated for actinomycin D, etoposide and staurosporine [32]. It is interesting to note that changes in $\Delta\Psi_m$ were in parallel with ability to induced apoptosis by C-1305 estimated by several assays (e.g. internuclesomal DNA fragmentation, appearance of sub-G1 population and Annexin V-positive cells). The collapse of $\Delta\Psi_m$ is a signature of the opening of the mitochondrial pores responsible for an uncoupling of the respiratory chain and efflux of small molecules (e.g. cytochrome *c*, calcium) and certain proteins including caspase-2 and -9 as well as the apoptosis-inducing factor (AIF), which can in turn stimulate the proteolytic activation of caspase-3 [16]. During apoptosis, the cellular level of the caspases greatly varies depending on the inducers and type of cell lines. In particular, activation of caspase-3 plays the central role in the executing stage of apoptosis [33,34]. Our study revealed that C-1305 treatment induced significant increase in number of cells with active caspase-3. After 72 h of incubation with C-1305, 65% of MOLT4 cells had active caspase-3, but in the case of HL60 cells only in 5% of cells populations caspase-3 was activated (Fig. 8, panel A).

We also determined the extent of PARP cleavage – preferential substrate for caspase-3 – by immunoblot analysis. In MOLT4 cells treated with C-1305, PARP proteolysis and the activation of caspase-3 were observed concomitantly with the dissipation of $\Delta\Psi_m$. Compared to MOLT4 cells, the small

population of HL60 cells with dissipated mitochondrial inner potential ($\Delta\Psi_m$) coincided well with the small population of the cells with active caspase-3 and with the efficiency of PARP cleavage (Fig. 8, panel B). Because in both cells types the activation of caspase-3 was observed concomitantly with the dissipation of $\Delta\Psi_m$, this might suggest the putative role of the mitochondrial pathway in C-1305-induced apoptosis.

The damage of mitochondria and associated ATP depletion appears to be a critical step of the apoptotic process [15]. Thus, we evaluated the effect of C-1305 on the ATP level in MOLT4 and HL60 cells. We observed a decrease of ATP level after 12 h of incubation with the drug and this effect was further intensified after prolonged incubation time (Fig. 8, panel C). In MOLT4 cells the depletion of ATP correlated with the decrease of $\Delta\Psi_m$ and activation of caspase-3. In HL60 cells, despite of evident depletion of cellular ATP content, we observed reduction of $\Delta\Psi_m$ as well as the increase in caspase-3 activity, only in part of cell population. Disruption of ATP levels by C-1305, despite of being a consequence of mitochondrial damage, may be also, in part, a consequence of the induction of a repair processes of damage DNA which resulted in induction of poly(ADP-ribose) synthesis followed by depletion of cellular NAD and ATP [21], but this needs further investigation. This could be important because in recent years only a limited interest of the role of ATP depletion in cell death was observed. The question whether ATP depletion is one of the causes or consequences of events leading to cell death is still open.

In summary, our data indicated that C-1305 at biologically relevant concentration, corresponding to EC_{90} values, induced cell cycle arrest in the G2/M phase of human leukemia cells, followed by apoptosis. In the case of lymphoblastic MOLT4 cells we observed massive death by apoptosis. Compared to MOLT4 cells, the capacity of HL60 cells to execute apoptosis after C-1305 treatment at equitoxic dose was significantly weaker, but very effective at higher concentration ($4\times$ EC_{90}). In both human leukemia cells exhibited the typical morphological changes associated with apoptosis: cell shrinkage, nuclear condensation, membrane blebbing, DNA fragmentation. In addition, apoptosis was mediated by caspase-3 activation, PARP cleavage, accompanied by the decrease of the mitochondrial transmembrane potential $\Delta\Psi_m$ and ATP depletion. These observations indicated that mitochondria-mediated processes may be involved in the induction of apoptosis of both leukemia cells treated with C-1305. Ability of C-1305 to induce cell cycle arrest at G2/M phase followed by very effective induction of apoptosis in tumor cells, give us an additional argument to consider this compound as a novel, potent and promising therapeutic agent against cancer.

Acknowledgments

This work was support by State Committee for Scientific Research (KBN), Poland, grant no. 4PO5A09017 and by Foundation for Development of Polish Pharmacy and Medicine (Polpharma), Poland, grant no. 014/2002. We also grateful to Gabriela Dzierżko from the group of professor Stefan Angielski, Department of Biochemistry, Medical University of Gdańsk, for expert technical assistance in determination of ATP level experiments.

REFERENCES

[1] Chołody MW, Martelli S, Konopa J. 8-Substituted 5-[(aminoalkyl)amino]-6H-v-triazolo[4,5,1-de]acridin-6-ones as potential antineoplastic agents. J Med Chem 1990;33:2852–6.
[2] Kuśnierczyk H, Chołody MW, ParadziejŠLukowicz J, Radzikowski Cz, Konopa J. Experimental antitumor activity and toxicity of the selected triazolo- and imidazoacridinones. Arch Immunol Ther Exp 1994;42: 415–23.
[3] Lemke K, Poindessous V, Składanowski A, Larsen AK. The antitumor triazoloacridone C-1305 is a topoisomerase II poison with unusual properties. Mol Pharmacol 2004;66:1035–42.
[4] Lemke K, Larsen AK, Konopa J, Składanowski A. Specific inhibition of the growth-associated alpha isoform of topoisomerase II by the novel anticancer triazoloacridinone C-1305. Eur J Cancer 2002;38(Suppl):45.
[5] Węsierska-Gądek J, Schloffer D, Gueorguieva M, Uhl M, Składanowski A. Increased susceptibility of poly(ADP-ribose) polymerase-1 knockout cells to antitumor triazoloacridone C-1305 is associated with permanent G2 cell cycle arrest. Cancer Res 2004;64:4487–97.
[6] Wurzer G, Herceg Z, Węsierska-Gądek J. Increased resistance to anticancer therapy of mouse cells lacking the poly(ADP-ribose) polymerase attributable to up-regulation of the multidrug resistance gene product P-glycoprotein. Cancer Res 2000;60:4238–44.
[7] Konopa J, Koba M, Dyrcz A. Interstrand crosslinking of DNA by C-1311 (Symadex) and other imidazoacridinones. Proc Am Assoc Cancer Res 2005;46:1382.
[8] Składanowski A, Konopa J. Mitoxantrone and ametantrone induce interstrand cross-links in DNA of tumor cells. Br J Cancer 2000;82:1300–4.
[9] Koba M, Konopa J. Interaction of antitumor triazoloacridones with DNA. Proc Am Assoc Cancer Res 2002;43:959.
[10] Dunkern TR, Fritz G, Kaina B. Ultraviolet light-induced DANN damage triggers apoptosis in nucleotide excision repair-deficient cells via bcl-2 decline and caspase-3/-8 activation. Oncogene 2001;20:6026–38.
[11] Coultas L, Strasse A. The molecular control of DNA damage-induced cell death. Apoptosis 2000;5: 491–507.
[12] Garewal HS, Ahmann FR, Shifman RB, Celniker A. ATP assay: ability to distinguish cytostatic from cytocidal anticancer drug effects. J Natl Cancer Inst 1986;77:1039–45.
[13] Murray AW. Recycling the cell cycle: cyclins revisited. Cell 2004;116:221–34.
[14] Koopman G, Reutelingsperger C, Kuijten G, Keehnen R, Pals S, Van Oers M. Annexin V for flow cytometric detection of phosphatydilserine expression on B cells undergoing apoptosis. Blood 1994;84:1415–20.
[15] Kroemer G, Reed JC. Mitochondrial control of cell death. Nat Med 2000;6:513–9.
[16] Ly JD, Grubb DR, Lawen A. The mitochondrial membrane potential (deltapsi(m)) in apoptosis. Apoptosis 2003;8:115–28.
[17] Salvioli S, Ardizzoni A, Franceschi C, Cossarizza A. JC-1 but not DiOC6(3) or rhodamine 123 is a reliable fluorescent probe to assess $\Delta\Psi_m$ changes in intact cells: implications for studies on mitochondrial functionality during apoptosis. FEBS Lett 1997;411:77–82.
[18] Earnshaw WC, Martins LM, Kaufmann SH. Mammalian caspases: structure, activation, substrates, and function during apoptosis. Annu Rev Biochem 1999;68:383–424.

[19] Oliver FJ, de la Rubia G, Rolli V, Ruiz-Ruiz MC, de Murcia G, Murcia JM. Importance of poly-(ADP-ribose) polymerase and its cleavage in apoptosis. Lesson from an uncleavalable mutant. J Biol Chem 1998;273:33533–9.
[20] Kaufmann SH, Desnoyers S, Ottaviano Y, Davidson NE, Poirier GG. Specific proteolytic cleavage of poly-(ADP-ribose) polymerase: an early marker of chemotherapy-induced apoptosis. Cancer Res 1993;53:3976–85.
[21] D'Amours D, Desnoyers S, D'Silva I, Poirier GG. Poly(ADP-ribosyl)ation reactions in the regulation of nuclear fractions. Biochem J 1999;342:249–68.
[22] Kalwinsky DK, Look AT, Ducore J, Fridland A. Effects of the epipodophyllotoxin VP-16-213 on cell cycle traverse, DNA synthesis, and DNA strand size in culture of human leukemic lymphoblasts. Cancer Res 1983;43:1592–8.
[23] Konopa J. G2 block induced by DNA crosslinking agents and its possible consequences. Biochem Pharmacol 1988;37:2303–9.
[24] Składanowski A, Konopa J. Adriamycin and daunomycin induce programmed cell death (apoptosis) in tumor cells. Biochem Pharmacol 1993;46:375–82.
[25] Barry MA, Behnke CA, Eastman A. Activation of programmed cell death (apoptotis) by cisplatin, other anticancer drugs, toxins and hyperthermia. Biochem Pharmacol 1990;40:2353–62.
[26] Nurse P. Universal control mechanism regulating onset of M-phase. Nature 1990;344:503–8.
[27] Kerr JF, Wyllie AH, Currie AR. Apoptosis: a basic biological phenomenon with wide-ranging implications in tissue kinetics. Br J Cancer 1972;26:239–57.
[28] Rello S, Stockert JC, Moreno V, Gamez A, Pacheco M, Juarranz A, et al. Morphological criteria to distinguish cell death induced by apoptotic and necrotic treatments. Apoptosis 2005;10:201–8.
[29] Roninson IB, Brodue EV, Chang BD. If not apoptosis then what? Treatment-induced senescence and mitotic catastrophe in tumor cells. Drug Resist Updates 2001;4:303–13.
[30] Kerr JF, Winterford CM, Harmon BV. Apoptosis: its significance in cancer, and cancer therapy. Cancer 1994;73:2013–26.
[31] Bossy-Wetzel E, Green DR. Detection of apoptosis by annexin V labelling. In: Reed JC, editor. Methods in Enzymology, 322. New York: Academic Press; 2000. p. 15–8.
[32] Finucane DM, Waterhouse NJ, Amarante-Mendes GP, Cotter TG, Green DR. Collapse of the inner mitochondrial transmembrane potential is not required for apoptosis of HL60 cells. Exp Cell Res 1999;251:166–74.
[33] Cohen GM. Caspases: the executioners of apoptosis (Pt 1). Biochem J 1997;326:1–16.
[34] Los M, Stroh C, Janicke RU, Engels IH, Schultze-Osthoff K. Caspases: more than just killers? Trends Immunol 2001;22:31–4.